A new Fe 4 Co 4 soluble switchable nanomagnet encapsulating Cs +: enhancing the stability and redox flexibility and tuning the photomagnetic effect.

J.-R Jiménez, M. Tricoire, D. Garnier, L.-M. Chamoreau, J. von Bardeleben, Yves Journaux, Yanling Li, R. Lescouezec

A new $\{Fe_4Co_4\}$ soluble switchable nanomagnet encapsulating Cs^+: enhancing the stability, the redox flexibility and tuning the photomagnetic effect.

J.-R. Jiménez,[a] M. Tricoire,[a] D. Garnier,[b] L.-M. Chamoreau,[a] J. von Bardeleben,[c] Yves Journaux,[a] Yanling Li,[a] R. Lescouëzec[a]

We report a new cyanide-bridged $Cs\subset\{Fe_4Co_4\}$ box, a soluble model of photomagnetic Prussian blue analogues (PBAs). The Cs^+ ion has a high affinity for the box and can replace the K^+ ion in the preformed K-cube. The exchange is kinetically impeded at room temperature but is accelerated by heating and using the 18-crown-6 ether. The inserted Cs^+ confers a high robustness to the cube, which resists boiling as shown by variable-temperature NMR studies. The stability of this model complex in solution allows the probing of the electronic interaction between the alkali ion and the cyanide cage by using various techniques. These interactions are known to play a role in the photomagnetic behaviour of PBAs. Firstly, the ^{133}Cs NMR spectroscopy proves that there is an electronic communication between the encapsulated alkali ion and the cyanide cage. The measured up-field signal, observed at *ca* -200 ppm at 300 K, reveals that a certain amount of spin density is transferred through the bonds from the paramagnetic Co(II) ion to the encapsulated cation. Secondly, the cyclovoltammetric studies show that the nature of the inserted ions affect the redox properties of the cage and influence the electronic communication between the metal ions. However, the differences in the electrochemical properties of the K-cube and the Cs one remain moderate. As the switching properties are influenced by the redox potential of the Fe and Co centers, similar photomagnetic behaviour are observed, both of them being highly photomagnetic. This result strikingly contrasts with previous studies on the 3D polymeric PBAs where the PBAs with a high Cs^+ amount show poor photomagnetic behaviour. In that case cooperative behaviour likely influences the switching properties. Finally the EPR spectroscopy shows that the K-cube is more anisotropic than the Cs one. This difference is reflected in the changes occurring in the slow magnetic relaxation (Single Molecule Magnet behaviour) observed in the two cubes.

Dedicated to the 75th anniversary of Prof. Emeritus Michel Verdaguer

Introduction

In 1996, Sato *et al.* discovered that the Curie temperature in a FeCo Prussian Blue Analogue (PBA) of the formula $K_{1.2}Co_4[Fe(CN)_6]_{3.1}\cdot 15.4H_2O$ could be increased by a light irradiation.[1] This photomagnetic effect was ascribed to an Electron Transfer Coupled to a Spin Transition (ETCST), which converts $\{Fe^{II}_{LS}\text{-}CN\text{-}Co^{III}_{LS}\}$ diamagnetic pairs into $\{Fe^{III}_{LS}\text{-}CN\text{-}Co^{II}_{HS}\}$ paramagnetic ones. The paramagnetic metastable state can then relax optically or thermally. The ETCST phenomenon can also be induced by other stimuli such as a temperature change. However, it has been shown that the switchable properties of these FeCo PBAs strongly depends on their chemical composition, in particular, on the amount and nature of the intercalated alkali ion, which itself is correlated to their (microscopic) structure.[2-3] For example, the $Cs_4Co_4[Fe(CN)_6]_4$ which contains Cs^+ ions in each 8g tetrahedral site of the cubic structure, does not show any photomagnetic effect. In contrast, its analogue of the formula $Cs_{0.7}Co_4[Fe(CN)_6]_{2.9}\square_{1.1}$ (where $\square$ represents $[Fe(CN)_6]$ vacancies) shows a very efficient photomagnetic effect.[4] This striking difference has been associated with the presence of vacancies in the second example, which confers some flexibility to the PBA network. Indeed, the ETCST is accompanied by important structural changes in the cobalt coordination sphere where metal-ligand distances vary by ca. 0.18 Å. In the diamagnetic compound $Cs_4Co_4[Fe(CN)_6]_4$, the framework is believed to be stiff because of the absence of vacancies and the presence of Cs^+ ion in all the cubic unit cells. The ETCST phenomenon is also highly dependent on the nature of the alkali ion. In order to clarify this aspect, Bleuzen *et al.* studied a family of $A_2Co_4[Fe(CN)_6]_{3.3}\cdot 11H_2O$ (A = Na^+, Rb^+, Cs^+) PBAs. They showed that the photomagnetic effect is more efficient when the polarizing character of the alkali cation increases. Thus, the strongest photomagnetic effect was observed for the Na^+ analogue. The observed trend was correlated to the interaction between the alkali ion and the π cloud of the cyanides that tends to stabilize the metastable photo-induced state.[6] Many questions remain open. What is the nature of the intermediate excited states involved in the photo-conversion? How can the photo-conversion rate be improved? How can the relaxation temperature be increased? Overall, the rationalizing

[a] Sorbonne Universités, UPMC Paris 6, Institut Parisien de Chimie Moléculaire, CNRS UMR 8232, 4 place Jussieu, Paris 75252, France.
[b] Plateforme d'Analyse Chimique de Strasbourg-Illkirch – CNRS GDS 3670, Faculté de Pharmacie, Université de Strasbourg, 74 route du Rhin, F-67401 Illkirch cedex
[c] Institut des Nanosciences de Paris - CNRS UMR 7588, UPMC – Paris 6, Sorbonne Universités, 4 place Jussieu, F-75252 Paris cedex 05 France.
† Footnotes relating to the title and/or authors should appear here.
Electronic Supplementary Information (ESI) available: : Additional details on NMR, EPR, X-ray diffraction, magnetometry, UVvis and IR data. See DOI: 10.1039/x0xx00000x

of the magnetic properties in PBAs remains difficult because of their complex local structure. For example, various metal sites such as $\{M(NC)_4(H_2O)_2\}$, $\{M(NC)_5(H_2O)_1\}$, $\{M(NC)_3(H_2O)_3\}$ coexist in PBAs, even in stoichiometric phases.[8-9] Thus, their physical properties, such as the photomagnetism, result from the interaction of different metal sites. In the last decade, there has been a strong interest in the design of low dimensional systems, which could be used as molecular models to help understanding the ETCST phenomenon. The self-assembly strategy, based on the reaction of iron building blocks having a reduced number of cyanide ligands, $[Fe^{III}(L)(CN)_x]^{n-}$, and Co building blocks with a reduced number of labile site (S), $[Co^{II}(L')(S)_y]^{m+}$, has allowed the design of a wide range of low dimensional Fe-Co based materials.[10-12] A first $\{Fe_4Co_4\}^{4+}$ cyanide-bridged photomagnetic cube was investigated by Holmes, Mathonière and Clérac in 2008.[13] In this cationic complex, the metastable state exhibits a long lifetime and a high relaxation temperature, which is measured in magnetometry (*ca*. 200 K). The phenomenon was also observed in FeCo square complexes in 2010,[14-15] or in FeCo bimetallic complexes more recently.[16] Interestingly, beside the occurrence of the ETCST phenomenon, other interesting features can be obtained in low-dimensional cyanide-bridged systems, including a multi-redox stability,[17-18] the occurrence of slow magnetic relaxation,[19-21] and dielectric bistability associated with electron transfer.[22] An appealing feature of some of these low-dimensional systems is also their solubility. On one hand, the solubility facilitates the insertion of the functional units into hybrid systems in the perspective of designing advanced materials of molecular devices. On the other hand, it allows the execution of interesting solution studies to enlighten the electronic properties of the individual molecules. In this context, we recently reported a neutral $\{Fe_4Co_4\}$ cage encapsulating an alkali K^+ cation (**K-cube**)[23], which shows a photomagnetic effect similarly to the original $K_{1.2}Co_4[Fe(CN)_6]_{3.1}\cdot 15.4H_2O$ PBA. We showed that the cage is highly soluble and stable in CH_2Cl_2. In this contribution, we show that the encapsulated K^+ can be fully replaced by Cs^+ ions in solutions containing a caesium salt. We also describe the impact of the cation substitution on the chemical and physical properties of the $\{Fe_4Co_4\}$ molecular cube. Interestingly, the presence of the inserted Cs^+ ion confers a better stability in solution to the cube even at high temperatures. The insertion of the Cs^+ also leads to an improved redox flexibility of the Cs-box, which exhibits up to eight accessible redox states (instead of 6 for **K-cube**). Furthermore, the Cs^+ encapsulation does not lead to a disappearance of the photomagnetic effect, in contrast with what was observed in the three dimensional PBA phases containing high amount of intercalated caesium.

Results and discussion

Solid-state structure

The mixed-valence cube of the formula $Cs\subset\{[Fe^{II}(Tp)(CN)_3]_4[Co^{III}(^{pz}Tp)]_3[Co^{II}(^{pz}Tp)]\}\cdot 12CH_3CN$ (**Cs-cube**) was prepared by first reacting $[PPh_4][Fe^{III}(Tp)(CN)_3]$ with $Co^{II}(ClO_4)_2\cdot 6H_2O$ and $Na[^{pz}Tp]$ in the presence of $CsClO_4$ and then by recrystallizing the product from an acetonitrile solution (see details in ESI). Deep blue prismatic single crystals suitable for X-ray diffraction were obtained by slow evaporation of the acetonitrile solution.

Figure 1. (top) View of the X-ray structure of **Cs-cube (**recorded at 200 K). Thermal ellipsoids are drawn at the 50 % level (C: black; N: blue; B: orange). Lattice solvents and hydrogen atoms have been omitted for clarity. (Bottom) View of the octametallic core encapsulating Cs^+ (Fe^{II}: yellow; Co^{III}: violet; Co^{II}: blue).

The **Cs-cube** crystallizes in a triclinic phase ($P\bar{1}$, Z = 2).[23] Its structure was obtained at 200 K. It is made of $Cs\subset\{Fe_4Co_4\}$ cubic motifs and acetonitrile lattice molecules (instead of CH_2Cl_2 molecules in the recently reported **K-cube**). No chemical interactions were detected between the lattice acetonitrile and the terminal organic ligands surrounding the octametallic core. The shortest intermolecular metal-metal distance (ca. 9.0 Å) is found between the Co ions. In each cube, four iron and four cobalt atoms alternatively occupy the vertices to form a heterocubane structure. The metal ions are linked to each other by bridging cyanides along the cube

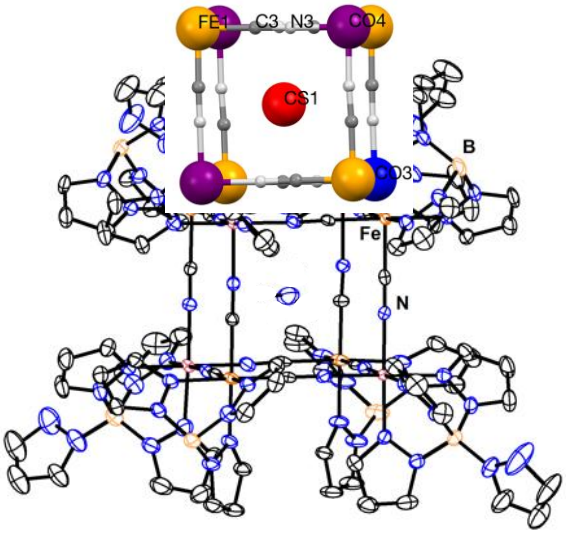

edges, the carbon atoms being always linked to the iron side. The Fe-CN-Co edge lengths are similar in both **K-cube**[23] and **Cs-cube**, with an average distance of 4.99 Å. However, the overall deviations from linearity of the Fe-C-N and Co-N-C links are smaller in the **Cs-cube** as compared to the **K-cube**. The Fe-C-N angle are almost linear here (*ca*. 178 ± 1°) whereas they show bigger deviations, ranging from 174.1(3)° to 178.4(3)°, in the **K-cube**. The Co-N-C angles also show less deviation in the **Cs-cube** (ranging from 174.1(3)° to 178.79(3)°) than in the **K-cube** (from 171.1(3)° to 178.8(3)°). These differences are coherent with the distortions observed in the Co^{II}_{HS} coordination sphere (see below). Overall, **Cs-cube** is less distorted than **K-cube**. This is also reflected in the location of the alkali ion inside the $\{Fe_4Co_4\}$ box. Because of its smaller size, the K^+ tends to be displaced toward a $\{Co(NC)_3\}$ corner of the cube, which is occupied by the Co(II) ions. The K···C and K···N distances of *ca*. 3.2-3.4 Å account for the small interactions with the three cyanide π systems. In the present **Cs-cube**, the alkali ion is located approximately at the centre of the cage. In fact, it is slightly closer to one of the faces. The Cs···C/N distances vary between 3.43-3.58 Å (with the closer face) and 3.50-3.66 Å

(with the opposite one). In addition, the Fe-CN-Co distances in the Cs^+ preferential face average 5.02 Å, while in the opposite one, the distances are slightly shorter, averaging 4.94 Å. This larger distance is caused by the presence of the Co^{II}_{HS} ion in one of the faces (ΔCo^{II}_{HS}-N is 0.2 Å larger than ΔCo^{III}_{LS}-N). Overall the interaction between the caesium ions and the twelve cyanide bridges likely contributes to the increased stability of the cage in solution at high temperatures (*vide infra*).

All the metal ions show a slightly distorted octahedral coordination sphere. They are coordinated in a *facial* mode to a scorpionate ligand (Tp or ^{pz}Tp) whereas the three other positions are occupied by the C atoms (for Fe) or the N atoms (for Co) of the cyanide bridges. Thus all coordination spheres exhibit a pseudo C_3 axis along the boron-metal axis. The Fe-C bond lengths fall in the range of 1.866(4)-1.900(4) Å and are similar to those previously reported for other $[Fe^{II}(Tp)(CN)_3]$} motifs.[24] The Co-N distances show less deviation than those observed in the **K-cube**. In contrast with the **K-cube** where one site was preferentially assigned to the Co(II) ions (with an occupancy of ½), two different pairs of cobalt sites can be distinguished from the XRD data of the C**s-cube**. One site exhibits an average Co-N bond length of 1.91 Å, which is typical of low-spin Co(III). The other site exhibits an average Co-N bond length of 1.98 Å, which corresponds to an average value between those expected for a HS Co(II) and a LS Co(III) ion. Thus, the unique HS Co(II) ion seems equally shared between two Co sites of the same face. The distortion of the Co(II) coordination spheres of the **Cs-cube** can be compared to that obtained in the **K-cube** (comparing the sites with a ½ occupancy). A significantly less distorted octahedral environment is found **in Cs-cube** (Σ = 18° compared to Σ = 28° for the **K-cube**).[25] It is worth noticing that the displacement of the Cs^+ ion toward this face probably reduces the local negative charge. The presence of a unique paramagnetic Co(II) ion is unambiguously revealed by other physical and chemical characterization. For example, the EPR spectrum of **Cs-cube** in frozen solution is typical of a magnetically isolated high-spin Co(II) ion (with I = 7/2) exhibiting an effective spin, S_{eff} = ½, at low temperature with an axial symmetry.[26-28] The g values remain close to those found in the **K-cube** ($g_{eff\perp}$ = 1.85 g_{effII} = 7.71) but the tensor shows a lower anisotropy ($g_{eff\perp}$ = 2.02 g_{effII} = 7.54). The remarkable variation of the $g_{eff\perp}$ values is linked to the conformation of the complex. The Cs^+ ion, which is more centred than the K^+ in the cage, causes a weaker local distortion of the "in-plane" cobalt coordination environment, which decreases the anisotropy of of g_{eff} (see ESI).

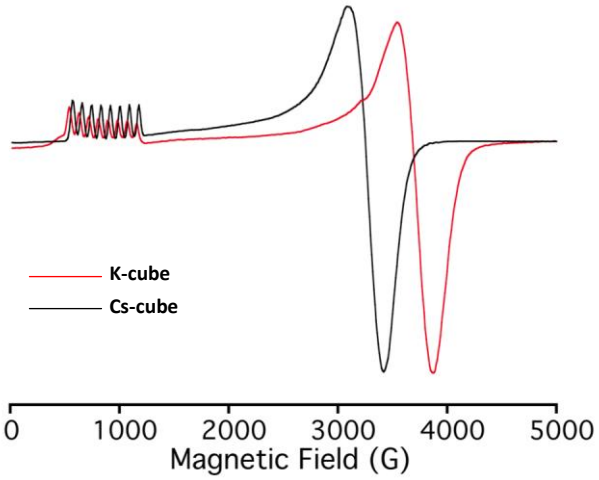

Figure 2. X-band EPR spectra of **K-cube** (red) and **Cs-cube** (black) in CH_2Cl_2 frozen solution at 4 K.

Solution studies

NMR and UV-vis studies

The ^{1}H-NMR spectrum of the **Cs-cube** has been recorded in CD_3CN. It shows strongly shifted signals, which appear at high field and low field, from – 86.7 to + 90.5 ppm at 300 K, and well-defined features located in the diamagnetic range (see ESI). Some of the signals are quite broad even though the resolution is improved in CD_3CN (present work) as compared to CD_2Cl_2 (our previous work). Thus more features are observed at room temperature. Moreover, unlike for the **K-cube** measured in CD_2Cl_2[23] we were able to detect the broad B-H protons (more details in ESI). The presence of a paramagnetic HS Co(II) in one of the vertices of the $\{Fe_4Co_4\}$ box leads to a C_{3V} molecular point-group. Considering the C_3 axis situated along the B-Co^{II}_{HS}-Cs direction, a set of 26 proton signals with an overall intensity corresponding to 88 protons (belonging to the pyrazolyl rings and the B-H of the Tp and ^{pz}Tp capping ligands) is expected. The peak assignment was done by considering the relative intensities of the signals and their chemical shifts: the closer the proton to the paramagnetic source is, the bigger the chemical shift appears. The half-width of the peaks can also be considered for the assignment, as the signals of protons close to the paramagnetic centre tend to broaden because of the fast magnetic relaxation due to the through-space dipolar interaction between the unpaired electron and the probed nucleus.[29] Overall, the ^{1}H NMR spectrum of the **Cs-cube** resembles that of the **K-cube**, although the signals are slightly less shifted. This trend is more visible on the most shifted proton signals and is likely correlated to the larger magnetic anisotropy observed in the **K-cube** as compared to that measured in the **Cs-cube** (see EPR spectra). Indeed, in paramagnetic species, the observed paramagnetic shift contains a pseudo-contact contribution (also called "dipolar shift"), δ^{pc}, which is directly correlated to the magnetic anisotropy (see below, equation 1). The bigger the anisotropy is, the bigger the pseudo-contact term is. As a consequence, the differences in the chemical shift values allow distinguishing both cubes in solution studies (*vide infra*). It is also worth underlying that the absence of other paramagnetic or diamagnetic signals (apart from those of solvent traces) accounts for the purity of the samples and the stability of the cubes at ambient temperature.

The ^{1}H NMR has also been used to probe the stability of the cage and the cation exchange in solution at different temperatures. No decomposition was observed in the case of the **Cs-cube** in the explored temperature range. In fact, upon slow heating (2 K/min) up to 350 K and further cooling to room temperature, the ^{1}H NMR signals of the the **Cs-cube** show a perfectly reversible temperature dependence (see ESI). Furthermore, the boiling of CD_3CN solution during 30 minutes does not affect the NMR spectrum. This behaviour contrasts with that of the **K-cube,** which shows some decomposition upon heating up to 80°C (see ESI). Overall, these NMR experiments demonstrate that the inserted Cs^+ ion confers a higher stability to the $\{Fe_4Co_4\}$ cage.

The **Cs-cube** can be directly prepared by using a caesium salt in the reaction medium (following the synthetic procedure mentioned above) but it can also be obtained from the **K-cube** by replacing the K^+ by Cs^+**.** However, the ^{1}H NMR experiments realized on solution containing **K-cube** and Cs salts show that the cation exchange is kinetically unfavourable. At room temperature, and even at 50°C, only traces of the **Cs-cube** were observed after several days (see ESI). In contrast, the experiments carried out at 65°C show a significant exchange in approximately 32 hours (about 60% of **Cs-cube**). The insertion of 18-crown-6-ether (18-C-6), under the same experimental conditions, allows an acceleration of the cation exchange. A full exchange between K^+ and Cs^+ is thus observed after 32 hours.

This points out the fact that the limiting step for the cation exchange involves the K^+ loss. The slow K^+-by-Cs^+ exchange observed here contrasts with the rapid exchange observed by Rauchfuss *et al*., within similar cyanide-bridged Co_8 and Rh_4Co_4 organometallic cages.[30,31] This difference is correlated to a higher inertia of our neutral **K-cube,** which contains only one labile Co(II) ion (*versus* four labile ions in the Rauchfuss cubes). Moreover, in order to confirm the better template effect of the Cs^+ ion, the synthesis of the cube was conducted in the presence of equimolar amounts of Cs^+ and K^+. The resulting products were isolated 3 minutes after the addition of the mixture of alkali salts and only the **Cs-cube** was identified by NMR spectroscopy.

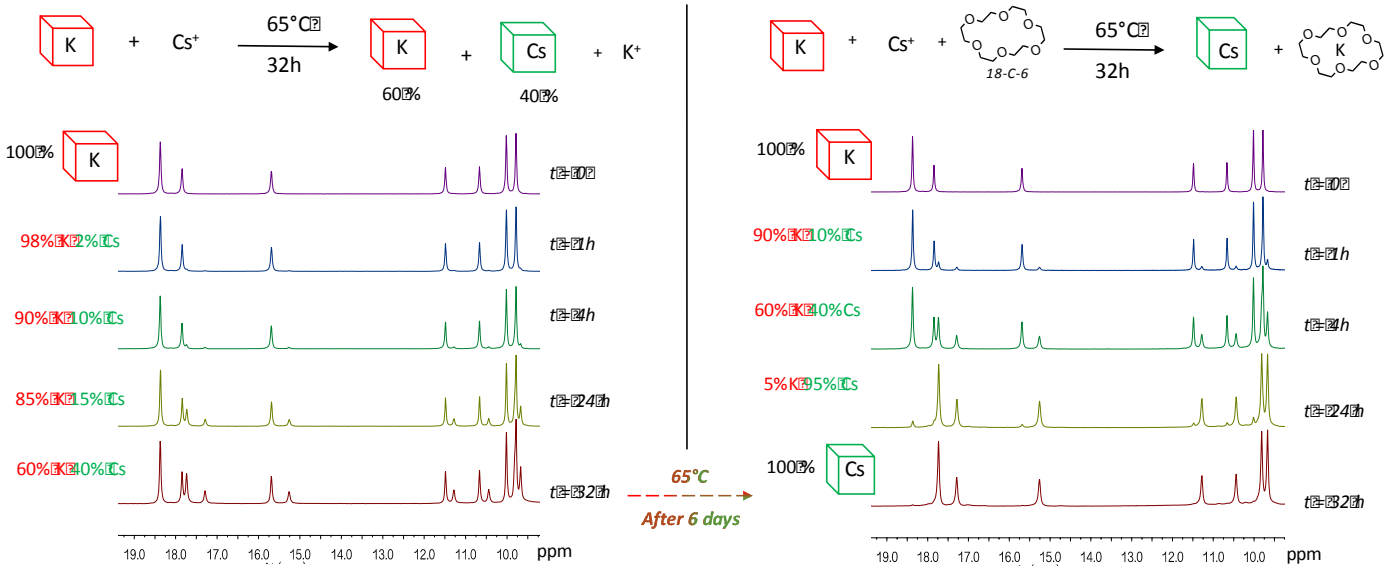

Figure 3. $K^+$by-Cs^+ exchange followed by ^{1}H-NMR (400 MHz) in CD_3CN at 65°C and at different times (0, 1, 4, 24 and 32h) in absence (left) and in presence (Right) of 18-C-6. The full exchange is obtained after 6 days in absence of 18-C-6, while it is observed after 32 h in presence of 18-C-6.

The UV-Vis absorption studies in acetonitrile solution (10^{-4} M) confirm the relative robustness of the **Cs-cube** compared to the **K-cube**. A broad absorption band centred at *ca*. 630 nm is observed in both species (see ESI). This absorption is assigned to the $Fe^{II}Co^{III}$ charge transfer band as previously observed in other molecular FeCo charge transfer systems.[32,33] Upon heating the **K-cube** solution, this band disappears and the blue solution turns yellow (see ESI). The colour change is irreversible and accounts for a decomposition of the **K-cube**. In contrast, the $Fe^{II}Co^{III}$ charge transfer band persists in the **Cs-cube** solution, although its intensity slightly decreases upon heating. The same result was obtained in butyronitrile solution, by heating up to *ca*. 110°C. In conclusion, the ^{1}H NMR and UV-vis spectroscopic results demonstrate that: (i) the K^+ ion can be efficiently replaced by the Cs^+ ion upon heating, (ii) the Cs^+ has a better template effect as compared to K^+ one, (ii) the $Cs\subset Fe_4Co_4$ cage is remarkably robust in organic solvents.

In addition to the ^{1}H NMR studies, the ^{133}Cs-NMR spectrum was also recorded in CD_3CN at 298 K (Figure 3). Beside structural analysis, interesting information can be obtained from this experiment. Although ^{133}Cs is a quadrupolar nucleus (I = 7/2), its very small quadrupolar coupling constant can lead to well-defined features in solution NMR. In the present case, a unique narrow signal is observed. This corroborates the purity and integrity of the **Cs-cube** in solution at room temperature and this indicates that only one Cs^+ site is observed in the molecules in solution.

The unique signal is remarkably shifted and it appears at – 236 ppm at 300 K, out of the ^{133}Cs diamagnetic range (*vs.* $CsNO_3$; $\delta = 0$ ppm in D_2O). This high field signal confirms that the Cs^+ is encapsulated in the cage and senses the HS Co(II) ion. The measured chemical shift thus contains an important paramagnetic contribution, δ^{para}, which arises from two effects (inset, figure 4): (i) the electron-nucleus dipolar interaction, which is a through-space interaction, leading to the pseudo contact shift, δ^{pc}; (ii) the Fermi contact term, which arises from the propagation of the unpaired electrons from the paramagnetic source to the probed nucleus, through the bonds. This interaction leads to a contact term, δ^{con}.

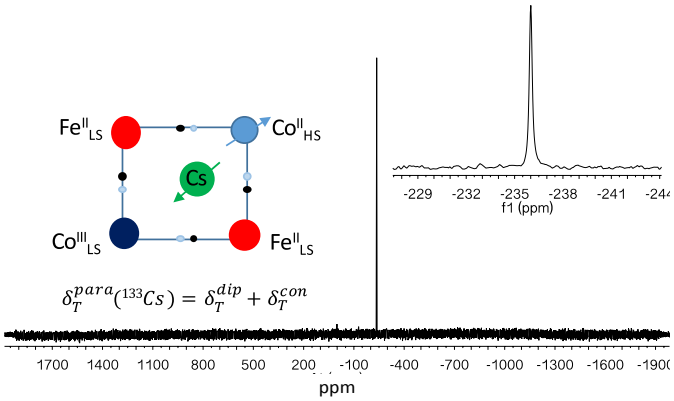

Figure 4. ^{133}Cs NMR spectrum of **Cs-cube** in CD_3CN at 300 K. Zoom on the observed signal (inset).

Recently, Köhler and Storcheva observed similar strongly-shifted ^{133}Cs signals in a series of paramagnetic PBAs of the formula $CsM^{II}[Co^{III}(CN)_6]$ (M^{II} = Ni, Co, Fe and Mn) PBAs.[34] In these systems, the Cs^+ is surrounded by four paramagnetic ions, and the strong shifts (observed down to -500 ppm) were ascribed to a through-bond spin transfer from the paramagnetic ions to the Cs^+ ion. The through-space dipolar interactions were neglected in this work. In the present case, a noticeable contribution of the electron-nucleus dipolar coupling is expected taking into account the strong magnetic anisotropy of the unique Co(II) paramagnetic source. Indeed, the dipolar contribution for a magnetically axial system is expressed following the equation:[35]

$$d_{PC} = \frac{m_0}{4p}\frac{bS(S+1)}{9kT}\frac{3\cos^2 q - 1}{r^3}(g_{//}^2 - g_\perp^2) \quad (1)$$

(β is the Bohr magneton, r is the distance between the magnetic source and the probed nucleus, θ is the angle between the main magnetic axis and the r direction). As the Cs^+ ion is approximatly localized on the magnetic axis (the C_3 axis of the cube), the geometric factor is positive ($\theta \approx 0°$) as is the resulting dipolar shift, δ^{pc}. The observed chemical shift, which is negative and strongly shifted to high fields, arises from an important negative contact contribution, δ^{con}. This negative contribution reflects a negative spin density on the Cs^+ ion.[34] In summary, the ^{133}Cs NMR signal brings an experimental proof of the occurrence of a through-bond comunication between the paramagnetic source and the Cs^+ ion. This communication occurs either directly through the valence orbital of the Cs^+ and the Co(II) ions, as suggested by Köhler *et col.*, or indirectly through the π orbital of the cyanide where the unpaired electron is delocalized.[36]

Cyclic voltammetry studies

In order to investigate the impact of the encapsulated Cs^+ ion on the electronic properties of the $\{Fe_4Co_4\}$ box, we have investigated the cyclic-voltammetry (CV) of the **Cs-cube** and and compared the results with the CV of the **K-cube**. The cyclic-voltamogramm of the **Cs-cube** measured in dichloromethane solution shows 7 oxidation waves (figure 5). The first oxidation wave located at -0.2 V (versus ferrocene) corresponds to the oxidation of the HS Co^{II} ion. The system looks irreversible as the corresponding reduction wave is shifted to lower potential, at -0.6V, and is broaden (see ESI). This behaviour is typical of slow redox systems where the electron transfer is associated with a spin transition on the metal complex. In the present case, the HS Co(II) center is oxidized in LS Co(III). This induces a strong structural rearrangement in the cobalt coordination sphere (ΔCo-N ≈ 0.18 Å) and a strong shift in the oxidation/reduction wave (the electron transfer can be fast on the electrochemical time scale but the structural rearrangement is slow). Such features have been observed for example in other slow redox systems such as the mononuclear Co(II) complexes containing scorpionate ligands similar to the Tp and ^{pz}Tp and also in the **K-cube**.[37,38] The four waves located at higher potential correspond to the quasi-reversible oxidation of the $Fe^{II/III}$ ions: $Fe^{II}_3Fe^{III}Co^{III}_4$ $E°_{1/2}$ = 0.36 V; $Fe^{II}_2Fe^{III}_2Co^{III}_4$ $E°_{1/2}$ = 0.47 V; $Fe^{II}Fe^{III}_3Co^{III}_4$ $E°_{1/2}$ = 0.65 V; $Fe^{III}_4Co^{III}_4$ $E°_{1/2}$ = 0.86 V (*versus* ferrocene). These redox potentials are centred at the same average potential, 0.575 V, in the **K-cube** and in the **Cs-cube**, however they appear in a slightly broader range for the **Cs-cube**. This difference can be quantified by comparing the comproportionation constants, K_c, which reflect the relative stability of the mixed valence states with respect to its (monovalent) reduced and oxidation forms. The comproportionation constant is calculated through the expression K_c = exp(FΔE/RT), where ΔE is the difference between successive oxidation waves. ΔE values of 0.13, 0.15 and 0.17 C lead to K_c values of 157, 343 and 750 for $\{Fe^{II}_3Fe^{III}Co^{III}_4\}^+$, $\{Fe^{II}_2Fe^{III}_2Co^{III}_4\}^{2+}$ and $\{Fe^{II}Fe^{III}_3Co^{III}_4\}^{3+}$ in the **Cs-cube**, meanwhile, higher values, of 307, 1030 and 3566 are found for the **K-cube**. This measurement highlights the small but noticeable influence of the nature of the alkali cation on the electronic communication between the metal ion through the cyanide bridges.[39-40] The weaker separation between the successive redox waves of the iron ions and the lower K_c values measured in the **Cs-cube** account for a weaker electronic communication between the metal ions when the K^+ ion is replaced by the Cs^+ one.

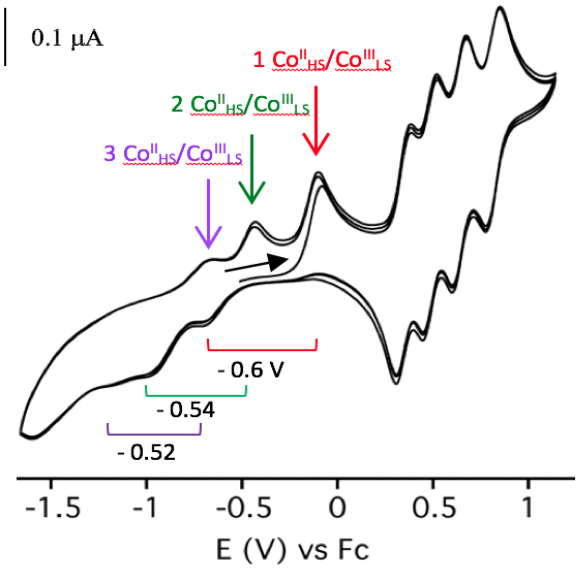

Figure 5. Cyclic voltammogram of the **Cs-cube** in CH_2Cl_2 (vs. Fc/Fc^+). $[Bu_4N][PF_6]$ 0.1 M, scan rate 100 mV s^{-1} WE: C, CE: Pt, Ref.E: ECS

	$E_{1/2}$ ($1Fe^{III/II}$)	$E_{1/2}$ ($2Fe^{III/II}$)	$E_{1/2}$ ($3Fe^{III/II}$)	$E_{1/2}$ ($4Fe^{III/II}$)
K-cube	0.32 V	0.47 V	0.65 V	0.86 V
Cs-cube	0.36 V	0.49 V	0.64 V	0.81 V

Table 1. Redox potential, $E_{1/2}$, for the successive Fe^{II}/Fe^{III} oxidation waves in the **K-cube** and **Cs-Cube**

Another striking difference between the two cubes is the occurrence of additional slow redox waves upon reduction in the **Cs-cube** (Figure 5). Whereas the **K-cube** shows only one slow redox wave corresponding to the HS Co(II) ion, two additional slow redox processes ascribed to two other cobalt ions are observed in the **Cs-cube** (see details in ESI). Thus, the encapsulated Cs^+ ion does not only confer a greater chemical stability to the $\{Fe^{II}_4Co^{II}Co^{III}_3\}$ box (*vide supra*) but also a higher redox flexibility, as eight redox accessible states are observed instead of six in the **K-cube**. The fourth cobalt centres cannot be reduced in the present experimental conditions, and the cube shows an irreversible redox process at ca. -1.5 V (details in ESI).

Solid state magnetic properties

Magnetic and photomagnetic properties

The temperature variation of the $\chi_M T$ is similar to those observed in the **K-cube** and is coherent with the presence of only one high-spin Co(II) paramagnetic ion per molecule. The magnetic data between 2 and 300 K can be simulated (using the PHI software),[41] and the best fit leads to a set of values which is similar to that obtained for the **K-cube** with a good agreement factor: λ = -143 cm^{-1}, α = 0.77, Δ = -922 cm^{-1} (where λ is the spin-orbit coupling, α is the reduction factor, Δ is the axial distorsion).[42] Interestingly, the slight and gradual increase of the $\chi_M T$ value observed above 350 K is the onset of a thermally-induced ETCST (see ESI). Its gradual aspect is coherent with the absence of remarkable intermolecular interactions between the cubes in the crystal lattice.

The photomagnetic properties were probed using an 808 nm laser diode of moderate power (5mW/cm^2). The **Cs-cube** shows a significant photomagnetic effect at 20 K. Indeed, upon irradiation, the paramagnetic signal quickly increases and reaches a saturation value of *ca*. $\chi_M T$ = 12.8 cm^3 mol^{-1} K after 20 minutes (figure 6). This value is higher than that observed for the **K-cube** (*ca*. 10 cm^3 mol^{-1} K) and could indicate a better conversion rate of the diamagnetic pairs into the paramagnetic ones. However, the magnetic exchange interaction through the cyanide bridge (and the spin-orbit coupling) may be different in the metastable states of the **K-cube** and the **Cs-cube** (because of structural differences) and thus impact their $\chi_M T$ values. It is thus difficult to make a conclusion about the relative efficiency of the photomagnetic effect. The increase of the $\chi_M T$ value before and after irradiation can also be compared to that measured in the related $\{Fe_4Co_4\}^{4+}$ cationic cube (*ca.* 12 cm^3 mol^{-1} K) where a full conversion was reported.[13] The increase in the **Cs-cube** is inferior (*ca.* 10 cm^3 mol^{-1} K) but only three $\{Fe^{II}_{LS}$-CN-$Co^{III}_{LS}\}$ vertices can be converted into three (Fe^{III}_{LS}-CN-Co^{II}_{HS}) paramagnetic pairs, because of the presence of the paramagnetic Co(II) ion in the ground state. Overall, the increase in both cubes are comparable. Although advanced physical measurements are needed to precisely measure the efficiency of the photo-induced electron transfer, these comparisons point to the occurrence of an efficient photo-induced ETCST effect. This strikingly contrasts with the absence of photomagnetic effect observed in the FeCo PBAs containing high amount of intercalated Cs^+. This difference is likely related to the structure of the materials. In the $Cs_4Co_4[Fe(CN)_6]_4$ PBA, there are no vacancies and the stiffness of the network likely impedes the structural reorganisation accompanying the ETCST. Here, the molecular cubes are well isolated from each other (see above) and there is likely no such structural constraint.

It is also worth noticing that the photo-induced metastable state in the **Cs-cube** persists up to T_{relax} ≈ 70 K, a value slightly inferior to that measured in the **K-cube** (T_{relax} ≈ 80 K, in the same experimental conditions). This observation is consistent with the results previously obtained in FeCo PBAs. Indeed Bleuzen *et coll.* showed that small alkali ions tend to stabilize the photo-induced paramagnetic pairs.[6] In summary, the Cs^+ ion leads to a reduced metastable time life (a reduce T_{relax}) as for the PBA, but it does not alter the photoconversion, in contrast with the situation observed in FeCo photomagnetic PBAs.

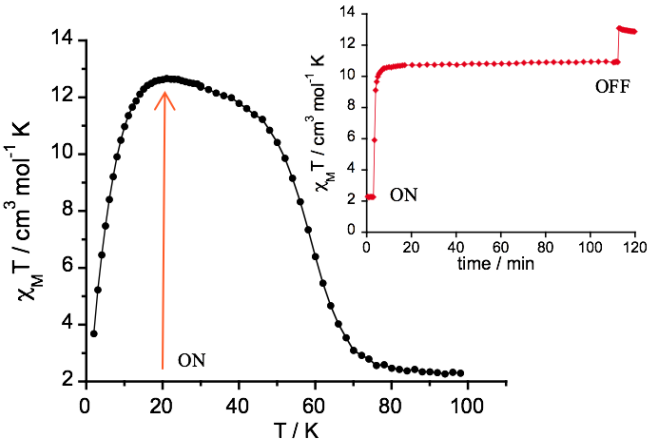

Figure 6. $\chi_M T$ *vs* *T* curve of the **Cs-cube** obtained after irradiation at 808 nm at 20 K during 2 h. Inset: time dependence of $\chi_M T$ of the **Cs-cube** at 20 K under irradiation at 808 nm (5mW/cm^2).

Single ion magnet (SIM) behaviour

In order to probe the dynamics of the magnetization, *AC* magnetic susceptibility was recorded as a function of temperature, field and frequency. At first the field dependent multifrequency AC measurements were performed at a very low temperature (3 K) to find the optimum static magnetic field giving the highest relaxation time. Then thermal variations of the AC magnetization were measured at different frequencies under the optimized static field. The frequency-dependence for both in-phase and out-of-phase of the ac susceptibility was observed only in the presence of a static magnetic field. The *ac* out-of-phase susceptibility signal exhibits a frequency-dependent maximum. The **Cs-cube** thus shows typical field-induced single-ion magnet (SIM) behaviour below 10 K (see details in ESI). The Cole-Cole plots (figure 7) at the optimal field of 1800 Oe show semi-circular shapes and

Direct		Tunnel		Raman		Orbach	
A ($T^{-2}K^{-1}S^{-1}$)		B1/(1+B2 H^2)	m	C ($K^{-n}S^{-1}$)	n	τ_0 (S)	U_{eff} (cm^{-1})
Cs-cube	39.3	209	1.64	7.50	3.85	2.91× 10^{-8}	71
K-cube	70.3	292	1.44	1.23	4.67	3.30×10^{-10}	134

can be fitted using a generalized Debye model in order to obtain the temperature dependence of the relaxation time τ. The ln(τ) *vs* (1/T) curve shows strong deviation from linearity at high temperatures, which is correlated with the coexistence of Raman and Orbach relaxation pathways. The simplified Arrhenius law $\tau = \tau_0 \exp(U_{eff}/kT)$, which is often used to estimate the energy barrier (U_{eff}) and the relaxation rate in the high temperatures range, leads to erroneous values of U_{eff} (underestimated) and τ (overestimated). Due to the presence of multiple relaxation mechanisms, it is more adequate to model the data following the equation:

$$\tau^{-1} = AH^mT + B_1/(1 + B_2H^2) + CT^n + \tau_0^{-1}\exp(-U_{eff}/kT) \qquad (2)$$

where the first and second terms correspond to direct and QTM (quantum tunnelling) relaxation mechanisms, the third and fourth represent the Orbach and Raman processes. Here we decided to adopt this approach to study the relaxation process and compare it to our previous results (see details in ESI). The obtained values, summarized in table 2, are similar to those reported for other Co(II) SIMs with a distorted

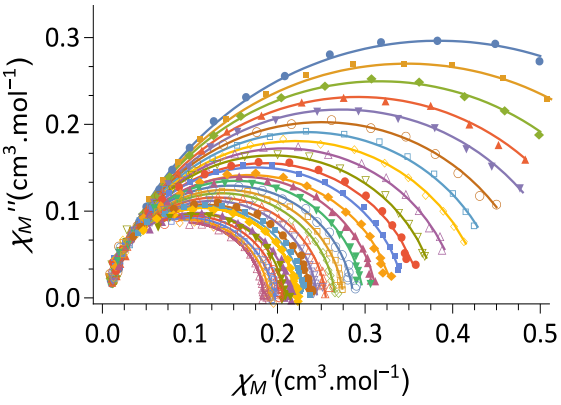

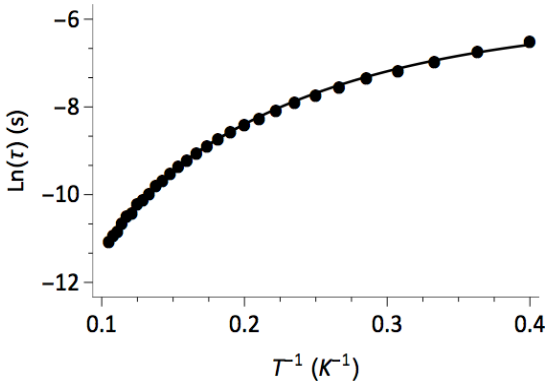

octahedral coordination environment.[43-44] The higher anisotropy of the cobalt(II) in the **K-cube** shows a remarkable agreement with the observed U_{eff} values. While the cobalt in the **Cs-cube** presents an energy barrier of 49.7 cm^{-1}, the slightly more distorted cobalt in **K-cube** shows an enhancement of U_{eff}, reaching a value of 90.7 cm^{-1}.

Figure 7. Cole-Cole plot of the **Cs-cube** between 2 and 10 K under a 1800 Oe magnetic field (top). Plot of the ln(τ) vs 1/T for the **Cs-cube.** (bottom). The solid lines represent the least square fitting of the data (see details in text and ESI).

Table 2. Values deduced from the fit of the relaxation processes and (see details in text and ESI).

Conclusions

A new multifunctional Cs⊂{Fe_4Co_4} cube has been obtained and its electronic, optical, magnetic and photomagnetic properties have been investigated. The complex can be obtained by direct reaction of the starting materials using the template effect of the cation. It can also be obtained by post-synthesis, replacing K^+ by Cs^+ within a preformed **K-cube**,

taking profit of the high affinity of the cage for the caesium ion. The exchange is kinetically blocked at room temperature but a full conversion is observed by heating. This study shows that these boxes are not "inert object" but can be opened and closed. The solution studies also showed that the Cs^+ ion confers a remarkable stability to the $\{Fe_4Co_4\}$ box, which stays stable even in boiling acetonitrile.

The robustness of the $Cs\subset\{Fe_4Co_4\}$ cube in organic solvents allows us to probe its electronic properties by using different solution studies. The interaction between the inserted cation and the molecular cyanide box is of particular interest as previous studies on PBAs materials tend to show that this interaction has an impact on the photomagnetic properties.

First of all, the strongly shifted ^{133}Cs chemical shift reveals the occurrence of an efficient spin transfer from the Co(II) paramagnetic ion of the $\{Fe_4Co_4\}$ box to the inserted caesium ion. The spin transfer can occur directly through the interaction of the Co(II) and Cs^+ valence orbitals as suggested previously by Köhler *et al*. It could also occur indirectly through the interaction of the Cs^+ ion with the π cloud of the cyanide ligands, which bear some unpaired electrons. In any case, the occurrence of one paramagnetic source in this model compound reveals this electronic interaction by tracking the spin transfer with NMR spectroscopy.

The interaction between the encapsulated alkali ion and the $\{Fe_4Co_4\}$ box is also revealed by cyclovotammetry. These experiments show that the electronic communication between the iron ions is affected by the nature of the cation (the communication being weaker for the **Cs-cube**). Moreover, the electrochemical studies showed that the encapsulated Cs^+ ion not only confers a better stability to the $\{Fe_4Co_4\}$ box but also a higher redox flexibility as eight redox states are accessible (instead of six in the **K-cube**). The $\{Fe_4Co_4\}$ box thus becomes stable in almost the full dichloromethane electrochemical window when the caesium ion is inserted. These experimental results are consistent with each other. The interaction between the caesium ion and the cyanide ligand obviously confers a higher chemical stability to the box, and it is likely responsible of the reduced electronic communication observed between the metal ions through the cyanide bridges. It may also reduce the donor ability of the cyanide ligand on the nitrogen side, leading thus to a stabilization of the reduced forms of the box.

Magnetic structural correlation can also be drawn between EPR experiments and the field-induced slow magnetic relaxation of the Co(II) ion. The bigger the axial anisotropy is, the larger the effective barrier U_{eff} is.

Finally, the influence of the K^+/Cs^+ substitution on the efficiency of the photo-induced electron-transfer appears to be less critical in the $\{Fe_4Co_4\}$ molecular model as compared to the three-dimensional FeCo PBAs. Here, the cubes remain quite isolated from each other, and no intermolecular interactions are observed in the crystal lattice. The structural reorganisation, which accompanies the ETCST phenomenon is thus less critical than in the cooperative three dimensional PBA networks (where a high amount of inserted Cs^+ ions confer a stiffness to the material). However, the nature of the cation impacts the relaxation temperature of the photo-induced metastable in a similar way as that observed for PBAs. In fact, the more polar cations, which may exhibit a stronger interaction with the π-cloud of some of the cyanide ligands, would stabilize the metastable states, leading thus to higher T_{relax}.

Overall, the study of these cubic complexes made way for the opportunity to evaluate some of the outcomes that were obtained from previous studies on the FeCo PBAs. As accurate electronic and structural information can be obtained on these molecular models, in the future we hope to reach a better understanding of the photomagnetic effect, in particular, the impact of the cyanide-ion interaction on the electronic, chemical and physical properties of these fascinating functional molecules. We are now investigating functional cages containing other cations.

Acknowledgements

This work was also supported by the Ministère de l'Enseignement et de la Recherche, the Centre National de la Recherche Scientifique and the Agence National de la Recherche (MoMa project, ANR-14-JTIC-0001).

Notes and references

1 O. Sato, T. Iyoda, A. Fujishima and K. Hashimoto, *Science*, 1996, **272**, 704.
2 C. Cartier dit Moulin, G. Champion, J. D. Cafun, M. A. Arrio and A. Bleuzen, Angew. Chem., Int. Ed., 2007, **46**, 1287;
3 V. Escax, A. Bleuzen, C. Cartier dit Moulin, F. Villain, A. Goujon, F. Varret and M. Verdaguer, *J. Am. Chem. Soc*., 2001, **123**, 12536;
4 O. Sato, Y. Einaga, A. Fujishima and K. Hashimoto, *Inorg. Chem.*, 1999, **38**, 4405.
5 A. Bleuzen, C. Lomenech, V. Escax, F. Villain, F. Varret, C. Cartier Dit Moulin and M. Verdaguer, *J. Am. Chem. Soc.*, 2000, **122**, 6648.
6 J. D. Cafun, G. Champion, M. A. Arrio, C. C. Dit Moulin and A. Bleuzen, *J. Am. Chem. Soc.*, 2010, **132**, 11552.
7 A. Bleuzen, V. Escax, A. Ferrier, F. Villain, M. Verdaguer, P. Münsch, J-P. Itié, *Angew. Chem*. 2004, **43**, 3728-3731
8 A. Flambard, F.-H. Köhler, R. Lescouëzec, *Angew. Chem. Int. Ed.* 2009, **48**, 1673 ;
9 A. Flambard, F.-H. Köhler, R. Lescouëzec, B. Revel, *Chem. Eur. J.* 2011*,* **17***,* 11567.
10 R. Lescouëzec, L. M. Toma, J. Vaissermann, M. Verdaguer, F. S. Delgado, C. Ruiz-Pérez, F. Lloret and M. Julve, *Coord. Chem. Rev.*, 2005, **249**, 2691.
11 C. P. Berlinguette, A. Dragulescu-Andrasi, A. Sieber, H. U. Güdel, C. Achim and K. R. Dunbar, *J. Am. Chem. Soc*., 2005, **127**, 6766.
12 D. Aguilà, Y. Prado, E. S. Koumousi, C. Mathonière and R. Clérac, *Chem. Soc. Rev.*, 2016, **45**, 203.
13 D. Li, R. Clérac, O. Roubeau, E. Harte C. Mathonière,R. Le Bris, and S. M. Holmes, *J. Am. Chem. Soc*., 2008, **130**, 1.
14 Y.-Z. Zhang, D.-F. Li, R. Clérac, M. Kalisz, C. Mathonière and S. M. Holmes, *Angew. Chem. Int. Ed.* 2010, **49**, 3752.
15 J. Mercurol, Y. Li, E. Pardo, O. Risset, M. Seuleiman, H. Rousselière, R. Lescouëzec and M. Julve, *Chem. Commun.* 2010, **46**, 8995
16 E. Koumousi, I.-R Jeon, Q. Gao, P. Deschabenoit, D.N. Woodruff, P. Merzeau, L. Buisson, X. Jia, D. Li, F. Volatron, C. Mathonière, R. Clérac, *J. Am. Chem. Soc*. 2014, **136**, 15461.
17 M. Nihei, M. Ui, N. Hoshino and H. Oshio, *Inorg. Chem. Comm*, 2008, **47**, 6106.

18 K. Mitsumoto, H. Nishikawa, G. N. Newton and H. Oshio, *Dalt. Trans.,* 2012, **41**, 13601
19 D. Li, S. Parkin, G. Wang, G. T. Yee, R. Clérac, W. Wernsdorfer and S. M. Holmes, *J. Am. Chem. Soc.*, 2006, **128**, 4214.
20 K. Mitsumoto, H. Nishikawa, G. N. Newton and H. Oshio, *Dalt. Trans.,* 2012, **41**, 13601.
21 J. Kim, S. Han, J.M. Lim, K-Y. Choi, H. Nojiri, B. J Suh., 2007, *Inorg. Chim. Acta*, **360**, 2647.
22 N. Hoshino, F. Iijima, G. N. Newton, N. Yoshida, T. Shiga, H. Nojiri, A. Nakao, R. Kumai, Y. Murakami, H. Oshio, *Nat. Chem*., 2012, 4.
23 D. Garnier, J.-R. Jiménez, Y. Li, J. von Bardeleben, Y. Journaux, T. Augenstein, E. M. B. Moos, M. T. Gamer, F. Breher and R. Lescouëzec*, Chem. Sci*., 2016, **7**, 4825.
24 A. Mondal, Y. Li, M. Seuleiman, M. Julve, L. Toupet, M.-L. Buron-Le Cointe and R. Lescouëzec, *J. Am. Chem. Soc*., 2013, **135**, 1653.
25 Σ is the sum of the deviation from 90° (in absolute values) of the twelve pseudo orthogonal N-Co-N angles of the octahedral coordination sphere (for comparison see ref. 24). Here, the Co^{II} crystallographic sites have a ½ occupancy, so Σ is underestimated. However the values can be compared as the occupancy is the same in both cubes.
26 P. Pietrzyk, M. Srebro, M. Radon, Z. Sojka and A. Michalak, J. *Phys. Chem. A*, 2011, **115**, 2316.
27 J. P. Jesson, J. Chem. Phys., 1966, **45**, 1049.
28 S. Stoll and A. Schweiger, *J. Magn. Reson*., 2006, **178**, 42.
29 Solution NMR of paramagnetic molecules, I. Bertini, C. Luchinat, G. Parigi, Elsevier, 2001.
30 J. L. Boyer, M. Ramesh, H. Yao, T. B. Rauchfuss and S. R. Wilson, *J. Am. Chem. Soc*. 2007, **129**, 1931.
31 J. L. Boyer, M. L. Kuhlman and T. B. Rauchfuss, *Acc. Chem. Res.* 2007, **40**, 4.
32 M. Nihei, Y. Sekine, N. Suganami, K. Nakazawa, A. Nakao, H. Nakao, Y. Murakami, H. Oshio, *J. Am. Chem. Soc*. 2011, **133**, 3592.
33 D. Siretanu, D. Li, L. Buisson, D. M. Bassani, S. M. Holmes, C. Mathonière, R. Clérac, *J. Am. Chem. Soc*. 2011, **17**, 11704.
34 F. H. Köhler and O. Storcheva, *Inorg. Chem*. 2015, **54**, 6801.
35 R.J. Kurland, B.R. McGarvey, *J. Mag. Res.* **1970**, *2*, 286.
36 F. H. Köhler, R. Lescouëzec, *Angew. Chem. Int. Ed*. 2004, **43**, 2571.
37 Kuzu, I. Krummenacher, I. J. Hewitt, Y. Lan, V. Mereacre, A. K. Powell, P. Höfer, J. Harmer and F. Breher, *Chem. Eur. J.,* 2009, 15, 4350.
38 J. R. Sheets and F. A. Schultz, *Polyhedron*, 2004, **23**, 1037
39 J. F. Endicott and Y. J. Chen, *Coord. Chem. Rev.*, 2013, **257**, 1676.
40 J.-P. Launay, *Chem. Soc. Rev.* 30 **2001** 386
41 N. F. Chilton, R. P. Anderson, L. D. Turner, A. Soncini and K. S. Murray, J. Comput. Chem., 2013, **11**, 1164
42 F. LLoret, M. Julve, J. Cano, R. Ruiz-Garcia and E. Pardo, *Inorg. Chim. Acta*, 2008, **361**, 3832.
43 J. Vallejo, I. Castro, R. R.-Garcia, J. Cano, M. Julve, F. LLoret, G. De Munno , W. Wernsdorfer and E. Pardo, *J. Am. Chem. Soc.* 2012, **134**, 15704
44 E. Colacio, J. Ruiz, E. Ruiz, E. Cremades, J. Krzystek, S. Carretta, J. Cano, T. Guidi, W. Wernsdorfer and E. Brechin, *Angew. Comm.* 2013, **52**, 9130
45 J.M. Zadrozny, M. Atanasov, A. M. Bryan, C.Y. Lin, B. D. Rekken, P. P. Power, F. Neese and J.R. Long, *Chem. Sci.* 2013, **4**, 125
46 Y. Rechkemmer, F. D. Breitgoff, M. v. d. Meer, M. Atanasov, M. Hakl, M. Orlita, P. Neugebauer, F. Neese, B. Sarkar, J. v. Slageren, *Nature Comm,* 2016, **7**, 10467
47 J. M Frost, K. L. Harriman and M. Murugesu, *Chem. Sci.,* 2016, **4**, 2470.